

# Development of Ballistic Limit Equations in Support of the Mars Sample Return Mission

William P. Schonberg<sup>(1)</sup>, Michael D. Squire<sup>(2)</sup>

<sup>(1)</sup> Civil Engineering Department, Missouri S&T, Rolla, MO 65409, USA; [wschon@mst.edu](mailto:wschon@mst.edu)

<sup>(2)</sup> NASA Engineering Safety Center, Hampton, VA 23681, USA; [michael.d.squire@nasa.gov](mailto:michael.d.squire@nasa.gov)

## Abstract

NASA and ESA are currently planning the Mars Sample Return campaign, comprising missions whose combined objective is to bring the first samples of Mars material back to Earth for detailed study. At present, the NASA-ESA plan is to return samples to Earth using three missions to be launched over the next 5-10 years. The final component, the Earth Entry System (EES), will bring the Mars samples back to the Earth, where it will land following safe entry through the Earth's atmosphere. There is a concern regarding the risk of biological contamination of the Earth's biosphere from returned Martian samples if, for example, the structural integrity of the EES were compromised during its return mission due to a perforation of a critical surface resulting from a high-speed meteoroid impact. To assess the risks associated with such an event, NASA is developing equations that predict the damage that various EES elements will sustain as a result of such an impact, as well as equations that predict whether or not a particular system will sustain a critical failure following such an impact. In this paper, we review recent progress in the development of such equations for the EES forebody and the EES aftbody, the two elements of the EES that are most exposed to the meteoroid environment. Limitations of the BLEs are also discussed, which can also be used to further inform the next steps in the BLE development.

## 1 Introduction

NASA and the European Space Agency (ESA) are currently planning the Mars Sample Return (MSR) campaign, comprising missions whose combined objective is to bring the first Mars samples back to Earth for detailed study [1]. Such an undertaking would allow more extensive analysis of the Mars material than currently possible in situ. At present, the NASA-ESA plan is to return samples to Earth using three missions:

- A sample collection mission (the Perseverance rover), launched in 2020 and currently operational on Mars collecting and caching Mars samples;
- A sample retrieval mission, to be launched in 2-3 years, which would contain a small rocket onto which the samples collected by Perseverance would be loaded using a robotic arm, and then launched off the Mars surface; and
- A return mission (the Earth Return Orbiter, or ERO), also to be launched in 2-3 years, which would secure the Mars samples in Mars orbit using its Capture, Containment, and Return System (CCRS), and then bring them back to Earth safely and securely in the early to mid-2030s.

The CCRS aboard the ERO would capture the Orbiting Sample container, orient it, and transfer it into a clean zone within its Earth Entry System (EES) for return to Earth. The ERO would then ferry the EES with the Mars samples back to the vicinity of Earth, where it would separate, enter the Earth's atmosphere, and land in the Utah desert. The EES would contain the Mars samples inside a cone-shaped vehicle with a heat shield for safe entry through the Earth's atmosphere.

There is, of course, the concern regarding the risk of biological contamination of the Earth's biosphere

from returned Martian samples. This could happen, for example, if the structural integrity of the EES were compromised during its return through damage to a critical surface resulting from a high-speed meteoroid impact. To assess the risks associated with such an event, NASA is developing equations that predict what level of damage the various EES elements will sustain as a result of such an impact.

Equations that are used to predict whether or not a particular system or structural element will sustain a critical failure following a hypervelocity impact are frequently referred to as ballistic limit equations, or BLEs. As such, BLEs are essential components of spacecraft system design as well as quantitative spacecraft risk assessments. In this paper, we review recent progress in the development of the BLEs for the EES forebody and the EES aftbody, the two elements of the EES that are most exposed to the meteoroid environment. We also present an overview of the processes used to develop such equations and offer some insights and suggestions into the next stages of development for these BLEs. Limitations of the BLEs are also discussed, which can be used to further inform the next steps in their development.

## **2 Ballistic Limit Equations**

### **2.1 General Comments**

A BLE is an equation that is used to predict whether or not a particular system or structural element will sustain a penetration or critical failure following a specific impact event. As such, BLEs are essential components of spacecraft system design as well as quantitative spacecraft risk assessments. There are two basic types of BLEs: those statistically derived from damage predictor equations and those using fail/no fail data points and fitting an equation to them.

The first kind of BLE is based on a damage predictor equation and is typically a statistically based curve-fit to damage measurements. An example of a damage predictor equation is one that predicts penetration depth into a structural element (e.g., thermal protection system, or TPS) in terms of impact parameters (impact velocity and obliquity), material properties (projectile material, TPS material), and geometries involved (TPS thickness, projectile dimensions, projectile shape). Once a critical or maximum acceptable damage level is identified (e.g., a maximum allowable penetration depth into a layer of TPS), the damage predictor equation is manipulated into a form in terms of all the other parameters that yields the particle diameter whose impact would result in the specified maximum acceptable damage level (i.e., the “critical diameter”). These parameters can either be incorporated into the BLE as variables, or a series of curves is created where each curve addresses a separate parameter (e.g., there may be separate curves for different projectile materials or impact obliquities).

The second kind of BLE is effectively based on a “hand-drawn” discriminant line. An example of a discriminant line BLE is one that separates regions of projectile diameter and impact velocity combinations that result in perforation of a dual-wall Whipple Shield from those that do not. These are the kinds of BLEs used for some of the shields on the International Space Station (ISS). Unlike damage predictor equations, discriminant line BLEs are not statistically derived curve-fits, but are simply lines of demarcation between regions where something either does or does not happen based on a specified failure criterion (e.g., perforation or non-perforation, or rear-wall spallation or no rear-wall spallation). An example of this type of BLE is the New-Nonoptimum (NNO) BLE, which is applicable for dual-wall structures such as those used in some locations on the ISS and which can be found in [2].

It is important to note that BLEs are specific for the structural element or system used in the test programs that generate the data upon which they are based. They are also a function of the criteria

used to define failure thresholds for the particular system or structural element under consideration. However, it is almost always the case that BLEs are needed beyond the testable regime, which is primarily limited by velocity. In such cases, assumptions are made regarding what is expected to happen at, for example, impact velocities far in excess of current test capabilities. Hydrocodes can be used to corroborate or modify BLEs under such conditions. However, hydrocode predictions can themselves be suspect because their own internal equations (e.g., equations of state) are based on test data.

## 2.2 Status of EES BLE Development

Figures 1 and 2 show a sketch of the EES forebody shield and TPS, and EES baseplate/aftbody—the elements of the EES for which bespoke BLEs have been developed.

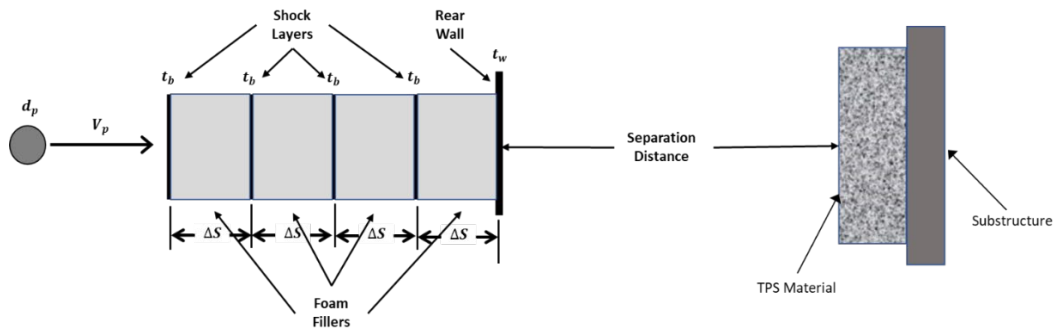


Fig. 1. Sketch of the EES Forebody Shield+TPS System (Elements and Distances Not to Scale)

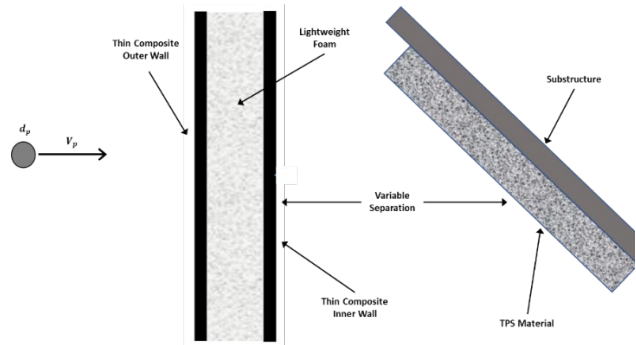


Fig. 2. Sketch of the EES Aftbody Shield+TPS System (Elements and Distances Not to Scale)

As the design of the EES and its protective shielding evolves, a suite of new BLEs is required to predict and assess the performance of candidate shield designs, structural wall systems, and any underlying layers of TPS anticipating damage from high-speed impacts by meteoroids or, nearer to the Earth, orbital debris. Table 1 summarizes the current status of the BLEs required for this purpose; an overview of some of the key features of several of these BLEs is presented in the next sections.

Table 1. Status of BLE Development for EES Elements

EES Region	Element	BLE Status
Forebody	Multi-shock shield (only)	Completed
	TPS (only)	Existing JSC equation
	Multi-shock shield + TPS (system)	Completed
Aftbody	Baseplate (only)	Preliminary
	TPS (only)	Completed
	Baseplate + TPS (system)	Not yet started

### 2.3 The Forebody Multi-Shock Shield (Only) BLE

The meteoroid shield that protects the EES forebody TPS consists of alternating layers of a shocking material and a foam filler, hence the term “multi-shock shield.” Each additional layer of both will increase the protective capability of the shield. The forebody multi-shock shield BLE (hereafter referred to as the “forebody shield BLE”) was developed by combining two previously developed multi-shock BLEs [2,3] into a single BLE, and then adjusting its coefficients and exponents so that the resulting BLE curves would fit penetration/no penetration (P/NP)<sup>1</sup> test results of candidate forebody shielding systems. Further adjustments to this BLE were then made so that it would also be applicable to additional forebody shielding configurations being considered using the results of SPHC<sup>2</sup> and ALE3D<sup>3</sup> hydrocode simulations. Throughout this process, checks were continually made to ensure that each new iteration of the forebody shield BLE coefficients and exponents would continue to yield the original multi-shock BLEs in [2,3] when the materials and geometries of those original shields were used in the BLE being developed for the forebody shield.

The forebody shield BLE has been further updated to include a variety of projectile materials including ice, aluminum, dunite, and iron. The most recent version of this BLE also has a much “flatter” form above 10 km/s (i.e., the rate of critical diameter decrease is lower as impact velocity increases beyond 10 km/s) when compared to the earlier version of BLE. This change was necessary so that the forebody shield BLE better fit the P/NP data generated at those higher impact velocities by the SPHC hydrocode. Details regarding the development of the forebody shield BLE can be found in [4].

Figure 3 shows a plot of the current forebody shield BLE for aluminum projectiles impacting one of the shield configurations used in its development (referred to hereafter as Layup #1, having 6 shock layers and 6 foam filler layers). Also shown in Fig. 3 are the SPHC P/NP data points for a variety of impact velocities between 7 km/s and 55 km/s, all at 30-deg impact obliquities. In this figure (and in subsequent figures), solid points represent SPHC runs that resulted in no perforation of the rear-most wall of the multi-shock shield (an NP result), while hollow data points represent runs in which it was perforated (a P result). As can be seen from this figure, the BLE falls, for the most part, exactly where it should: above the highest NP data point and below the lowest P data point for each simulated impact velocity.

Comparisons between BLE plots and SPHC P/NP predictions (as well as with test results at impact velocities near 7 km/s) for other candidate forebody shield configurations were found to be similar in their agreement levels, that is, most of the hollow (i.e., perforating) data points were seen to lie above the BLEs (where they should be), and most of the solid (i.e., non-perforating) data points were seen to lie below the BLEs (where they should be). There are some instances where there is a hollow data point below a BLE or a solid data point above a BLE. However, this kind of occasional flip-flop is not unusual in plots of the BLEs that model the P/NP response of multi-wall systems under hypervelocity impact because of the inherent stochastic nature of the phenomenologies associated with such impacts (see also, [5]).

---

<sup>1</sup> Traditionally, the term P/NP (i.e., penetration/no penetration) has represented either meeting or exceeding the defined failure criteria, which may or may not correspond to penetration or no penetration. It may correspond to other ways used to determine whether or not an impacted target has exceeded a defined damage threshold (e.g., depth of penetration). In this paper, P/NP will be used generically to indicate whether an impact event exceeded the damage criteria, regardless of how those criteria have been defined.

<sup>2</sup> SPHC = Smooth Particle Hydrocode

<sup>3</sup> ALE = Arbitrary Lagrangian-Eulerian

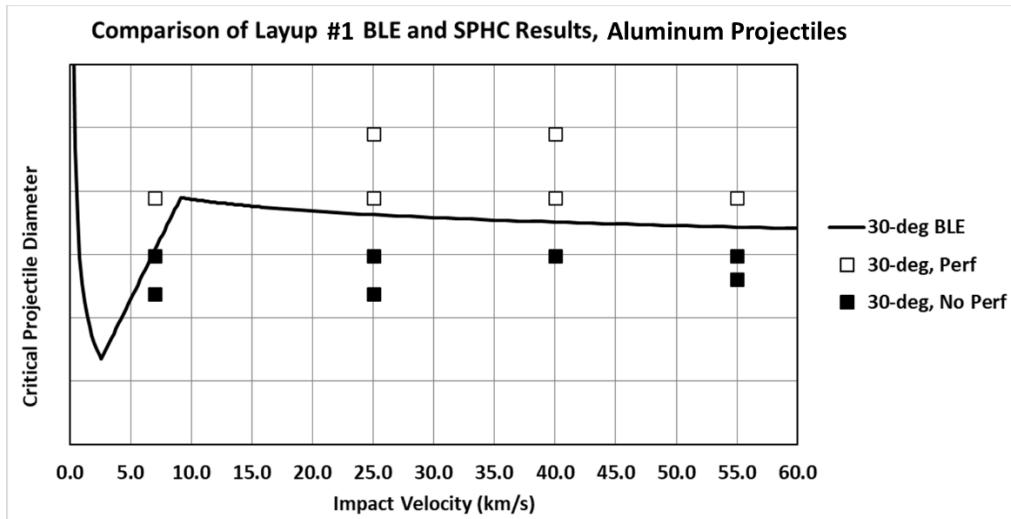


Fig. 3. Comparison of BLE plot and SPHC P/NP Simulation Results for Forebody Shield Layup #1; Impact Obliquity = 30°. The line is the BLE and the squares (both solid and open) are SPHC data points.

The inflection points at impact velocities at approximately 2.5 and 9 km/s give this curve the typical bucket shape characteristic of BLEs for multi-wall configurations. These changes in the shape of the BLE correspond to impact velocities where significant changes in the projectile's phenomenological response occur. For example, in this case, for velocities less than ~2.5 km/s, the projectile remains whole (or nearly so), so increased velocity up to 2.5 km/s will simply increase the kinetic energy of the projectile with no dispersal of the projectile as it exits the final shield layer. This translates into increased damage and decreased critical diameter. Above 2.5 km/s, increasing fragmentation of the projectile occurs, resulting in both energy loss in the fragmentation process and a dispersal of the energy over a wider area. The result is an increasingly larger projectile needed to perforate the shield as velocity increases; so, at ~2.5 km/s, the curve increases.

As the impact velocity continues to increase, projectile fragments liquefy, converting even more kinetic energy, until all projectile material has been melted. Beyond some impact velocity, here ~9 km/s, the impact is so energetic that the molten projectile fragments have an increased penetrating capability, so smaller projectiles are able to perforate the shield and the BLE curve decreases. The particular locations of these two inflection points depend on the materials of the projectile and the shield, as well as the impact obliquity angle. Additional information on the phenomenological changes that occur as impact velocity is increased can be found in [6].

In the end, a new, more general, BLE has been successfully developed for multi-shock shielding systems that compares favorably with hydrocode and impact test results. This expanded BLE is now applicable to multi-shock shield designs made with materials other than those that were used in its original development, thereby rendering it applicable to a wider class of spacecraft designs.

The applicability of the BLE has also been extended to include impact velocities beyond the testable regime and a much wider range of projectile materials. As a result, this more generalized form of the multi-shock shield BLE can be used in trade studies that are typically performed as part of efforts to select and optimize multi-shock shield designs for future spacecraft. Further refinement of the BLE functions and their parameters is expected to continue with new data from additional impact tests and numerical simulations.

## 2.4 Forebody Shield+TPS System BLE

The forebody shield+TPS system considered herein consists of a multi-shock shield and TPS standing off at a distance behind it; it does not include the supporting structure behind the TPS. The BLE developed for this system was also designed to be applicable across the full impact velocity range, that is, 1-60 km/s, and for impact obliquities 0°-45°. And the BLE was formulated to be sufficiently flexible so that it can be used for parametric and/or configuration design trade studies (i.e., it is written in terms of as many forebody shield and TPS system parameters as possible). Two versions of the BLE were developed—one with a 50% and the other with a 100% penetration depth as the failure criteria. In this manner, it can be used for the nose of the EES cone (where the failure criterion is currently 50% TPS penetration) as well as the EES frustrum (where the failure criterion is currently 100% TPS penetration).

The forebody shield+TPS system BLE was developed using the following process:

- Step Zero – Determine if the impacting projectile has perforated the forebody shield. This is accomplished using the forebody shield BLE described previously. If it has not, there can be no damage to the TPS. If it has, then we assume that some remnant of the original impact projectile will eventually impact the TPS
- Step One – If there is a forebody shield perforation (Step Zero), calculate the size and speed of the largest fragment exiting the forebody shield. This is accomplished by equivalencing the multilayer forebody shield with a single aluminum shield having a thickness that yields the same areal density as the forebody shield itself.
- Step Two – Using the size and speed characteristics of the largest perforating fragment, calculate the depth of penetration of that largest fragment into the TPS. This is accomplished using an existing empirical TPS penetration depth predictor equation.
- Step Three – Calibrate the penetration depth predictor model developed in Step Two against penetration depth values obtained by the SPHC hydrocode and testing. This is accomplished by modifying the existing TPS penetration depth predictor equation from Step Two so that it will yield TPS depth predictions that are closer to the values predicted by the hydrocodes and observed in testing.
- Step Four – Compare the calibrated TPS penetration depths against an allowable maximum TPS penetration depth value, and assign a P/NP (in this case, whether the allowed penetration depth has been exceeded) value to the characteristics of the original impacting projectile.
- Step Five – Repeat Steps One through Four for a range of projectile diameters, impact velocities, and trajectory obliquities to obtain the full BLE.

The forebody shield+TPS system BLE was originally developed using only aluminum projectiles in the SPHC simulations. That original form was modified based on test results at impact velocities near 7 km/s, and an additional term was added to account for projectile materials other than aluminum based on results obtained using SPHC and ALE3D hydrocodes. The most recent modifications to the forebody shield+TPS system BLE include terms that account for TPS thickness and stand-off distance between the rear of the shield and the forebody TPS.

Figures 4 and 5 show plots of the forebody shield+TPS system BLEs having the same forebody shield configuration as shown in Fig. 2 (i.e., Layup #1). Plots are presented for the two failure criteria being considered (50% TPS penetration and 100% TPS penetration) for projectile materials that simulate the materials of the most likely impactors. As can be seen from these figures, the BLE plots fall, again, for the most part exactly where they should—at a given impact velocity, they are above the highest NP data

point and below the lowest P data point. Comparisons between BLE plots and failure/non-failure predictions for other forebody shield+TPS system configurations were similar in their agreement levels. Finally, the hollow triangles represent data points where simulation results predicted penetration depths that were within 1 mm of the maximum allowable penetration depths. These data points could be considered as lying on or very near the ballistic limit for those particular impact conditions.

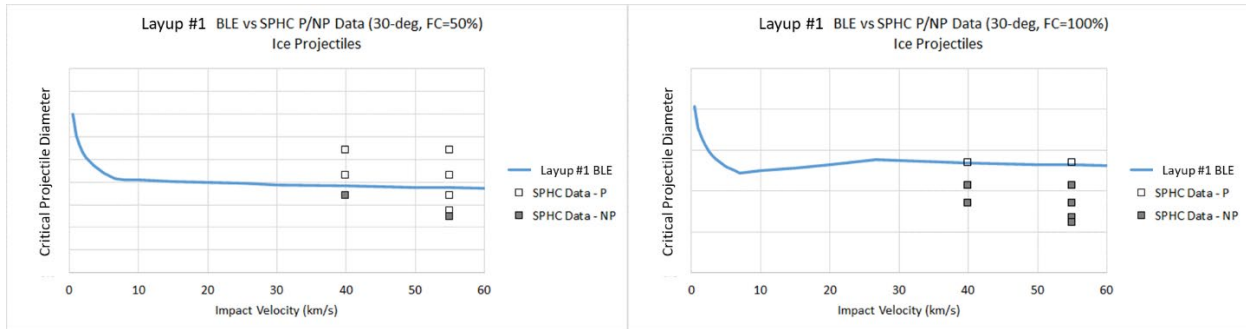


Fig. 4. Plots of Forebody Shield+TPS System BLEs for 50% and 100% TPS Penetration Depth Failure Criteria for Shield Layup #1 Ice Projectiles; Impact Obliquity = 30°.

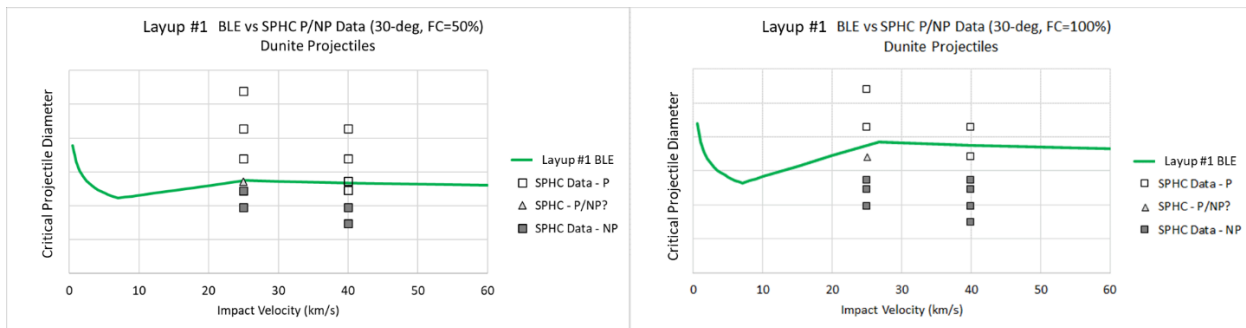


Fig. 5. Plots of Forebody Shield+TPS System BLEs for 50% and 100% TPS Penetration Depth Failure Criteria for Shield Layup #1; Dunite Projectiles; Impact Obliquity = 30°.

Although the forebody shield+TPS system BLE was developed using the parameters and configurations specified above, its current formulation is also sufficiently flexible to allow other combinations and numbers of alternating shock and foam layers. This is a particularly advantageous feature as it allows this BLE to be used for similar kinds of configurations not necessarily used in its development.

For example, this BLE also generated generally acceptable lines of demarcation between regimes of failure and non-failure when applied to a forebody shield+TPS system not used in its development (aka Layup #2, having 3 shock layers and 3 foam filler layers, and ~25% thicker than Layup #1). That is, in most cases, it was seen that the positioning of the BLE curve was such that most of the hollow “P” data points were above it, while at the same time, most of the solid “NP” data points were below it. Figures 6 and 7 show plots of this BLE for the 50% and 100% TPS penetration failure criteria for this configuration, respectively, again for projectile materials that simulate the density of the most likely impactors. The comparisons in Figures 6 and 7 show that the current BLE formulation appears to consistently represent failure modes based on current numerical impact simulations and experimental test results.

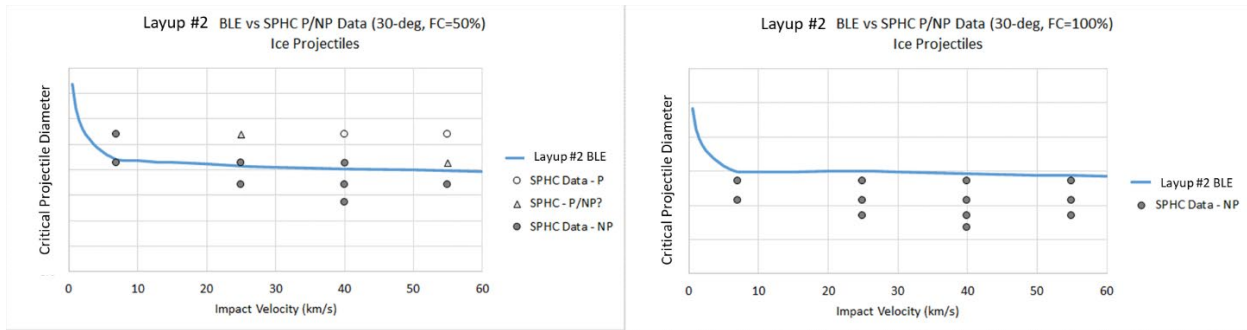


Fig. 6. Plots of Forebody Shield+TPS System BLEs for 50% and 100% TPS Penetration Depth Failure Criteria for Shield Layup #2; Ice Projectiles; Impact Obliquity = 30°.

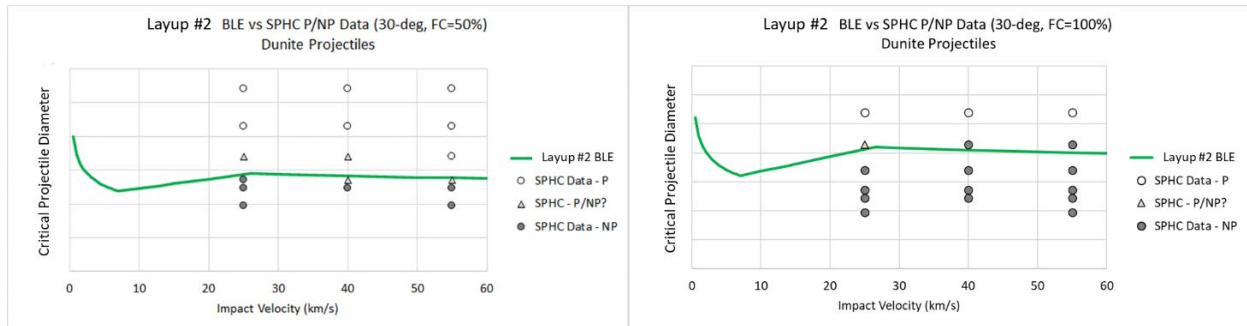


Fig. 7. Plots of Forebody Shield+TPS System BLEs for 50% and 100% TPS Penetration Depth Failure Criteria for Shield Layup #2; Dunite Projectiles; Impact Obliquity = 30°.

## 2.5 Aftbody Shield BLE

At present, there is only a minimal amount of data available regarding the P/NP performance of a micrometeoroid and orbital debris (MMOD) shield having the preliminary construction and composition of the EES baseplate, which functions as an aftbody shield. The baseplate comprises two thin composite plates standing off at a small distance from each other, with the space between them filled with a low-density non-metallic foam. On their own, these data are not sufficient for use in the development of the aftbody BLE. However, similar types of MMOD shield constructions have been examined (1) in test campaigns performed in the 1960s and 1970s, and (2) using the SPHC hydrocode simulation runs using a different low-density foam filler material.

Considering the availability of additional information as described above for constructions similar to the current aftbody MMOD shield design, the development of a preliminary aftbody shield BLE was undertaken. This BLE was obtained by modifying the coefficients in the NNO BLE so that the result is able correctly predict the P/NP response of an MMOD shield having a construction and composition similar to that of the aftbody shield. Several new terms were also added to take into account the trends observed in hydrocode simulations and in test results when non-aluminum projectiles and wall materials were used. Details regarding this development can be found in [7].

Figures 8 and 9 shows a plot of the original NNO BLE, the modified NNO BLE, and SPHC simulation results for whether or not perforation of an aftbody shield configuration has occurred. As can be seen from these figures, there is a marked improvement in the ability of the NNO BLE to predict perforation or non-perforation of a foam-filled dual-wall system once the changes to the NNO BLE noted above are introduced. For example, in Figure 8, some of the non-perforation data points are above the original



BLE, whereas they are all below the modified NNO BLE (they *should* all be below the BLE). And in Figure 9, most of the perforation data points are below the original NNO BLE, whereas when the modified version of the BLE is used, all of the perforation data points are above the BLE (which is where they should be). Although preliminary, the results indicate that the BLE accurately reflects the P/NP behavior seen in the SPHC results for the aftbody shield. As the aftbody shield design is finalized, this modified NNO BLE should be readily adaptable to any design changes or updates.

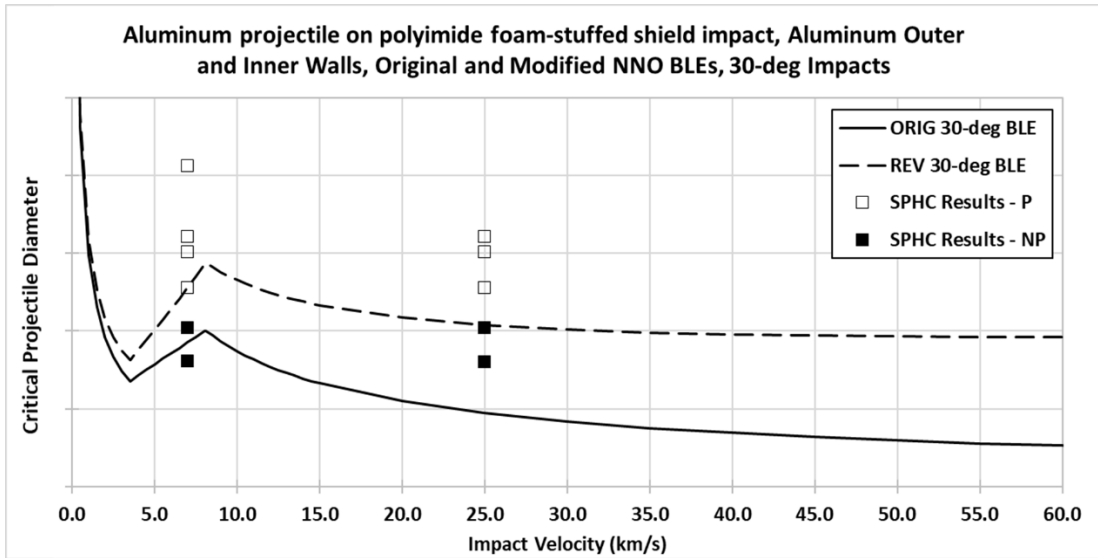


Fig. 8. Comparison of Original and Modified NNO BLEs against SPHC P/NP Data for Dual-Wall Systems with Aluminum Outer and Inner Walls

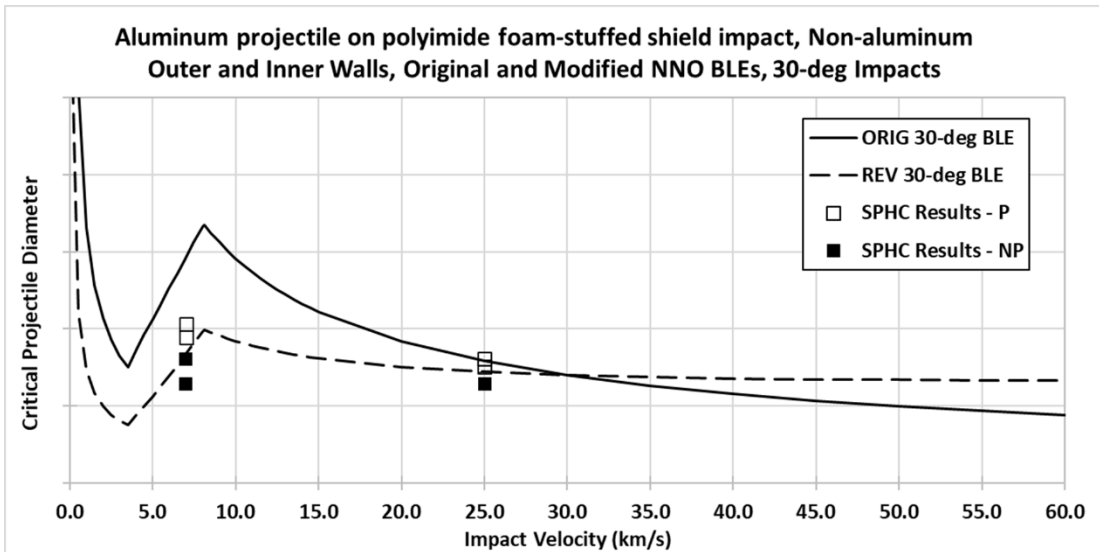


Fig. 9. Comparison of Original and Modified NNO BLEs against SPHC P/NP Data for Dual-Wall Systems with Non-Aluminum Outer and Inner Walls

## 2.6 Aftbody Shield+TPS System BLE

The development of this BLE will likely proceed using the process used in the development of the forebody shield+TPS system BLE. Work on this BLE is slated to begin once a preliminary design has been finalized and initial hydrocode simulation results are available for calibration.

## 2.7 Recent Developments

The CCRS Project has been considering alternative forebody shield configurations with the objective of saving mass while minimizing reductions in shield effectiveness. All of the proposed design trades retain the multi-shock configuration and vary materials, spacing, and foam filler between the layers. In addition, alternatives for the baseplate material including aluminum and multi-layer insulation are being considered. As of this writing, no design modifications have been selected by the Project, but if they are, the BLEs will need to be modified using new hydrocode and test data. These data are already being generated in support of the design trade studies currently underway. BLEs for the designs ultimately selected for flight will continue to be updated as more hydrocode and test data become available.

## 3 Conclusions

NASA and ESA are currently designing the Mars Sample Return campaign, which is intended to return samples to Earth using three missions to be launched over the next 5-10 years. As the final component, the Earth Entry System (EES), is intended bring the Mars samples back to the Earth, there is a concern regarding the risk of biological contamination of the Earth's biosphere from returned Martian samples if, for example, the structural integrity of the EES were compromised during its return mission by the perforation of a critical surface resulting from a high-speed meteoroid impact. To assess the risks associated with such an event, NASA is developing equations that predict the damage that various EES elements will sustain as a result of such an impact, as well as equations that predict whether or not a particular system will sustain a critical failure following such an impact. In this paper, we have reviewed recent progress in the development of such equations for the EES forebody and aftbody shields and TPS, the two elements of the EES that are most exposed to the meteoroid environment. Advantages as well as limitations of the BLEs have been discussed, which can be used in future efforts to inform the next steps in the development of such BLEs.

## 4 References

1. Cataldo, G., et al, "Mars Sample Return – An Overview of the Capture, Containment and Return System", Paper No. IAC-22-A3.3A.10, 73rd International Astronautical Congress, Paris, France, 18-22 September 2022.
2. Christiansen, E.L., "Design and Performance Equations for Advanced Meteoroid and Debris Shields", *International Journal of Impact Engineering*, Vol. 14, 1993, pp. 145-156.
3. Christiansen, E.L., Crews, J.L., Lear, D., and Lyons, F., "GLAST ACD Meteoroid/Debris Shielding: Initial Test and Analysis Results", 9 Nov 2021 (<https://www.slac.stanford.edu/>).
4. Schonberg, W.P., and Squire, M.D., "Toward a More Generalized Ballistic Limit Equation for Multi-Shock Shields", *Acta Astronautica*, submitted for publication, June, 2023.
5. Schonberg, W.P., and Compton, L.E., "Application of the NASA/JSC Whipple Shield Ballistic Limit Equations to Dual-Wall Targets under Hypervelocity Impact", *International Journal of Impact Engineering*, Vol. 35, 2008, pp. 1792-1798.
6. Hopkins, A.K., Lee, T.W., and Swift, H.F., "Material Phase Transformation Effects upon Performance of Spaced Bumper Systems", *Journal of Spacecraft*, Vol. 9, 1972, pp. 342-345.
7. Schonberg, W.P., "Extending the NNO Ballistic Limit Equation to Foam-Filled Dual Wall Systems", *Applied Sciences*, Vol. 13, 2023, Article No. 800.